

# The Complexation Chemistry of Cyclohexaamyloses. 4. Reactions of Cyclohexaamylose with Formic, Acetic, and Benzoic Acids and Their Conjugate Bases<sup>1-3</sup>

Robert I. Gelb, Lowell M. Schwartz, Robert F. Johnson, and Daniel A. Laufer\*

Contribution from the Department of Chemistry, University of Massachusetts at Boston, Boston, Massachusetts 02125. Received July 17, 1978

**Abstract:** pH potentiometric and <sup>13</sup>C NMR analyses of aqueous solutions of cyclohexaamylose and formic-formate, acetic-acetate, or benzoic-benzoate acid-base conjugate pairs indicate that only binary complexes form with each of the acids and with benzoate anion. Equilibrium constants for these complexation reactions are measured between 15 and 50 °C. These results yield thermodynamic parameters  $\Delta H^\circ$  and  $\Delta S^\circ$  for each complex formation. Interpretation of <sup>13</sup>C NMR resonances of cyclohexaamylose and substrate carbons of the various complexes indicates preferential binding of the acids within the narrow zone and of the benzoate anion within the wide zone of the cyclohexaamylose cavity.

In previous articles of this series we have studied complexes of 4-biphenylcarboxylate and *p*-methylcinnamate anions with both cyclohexaamylose<sup>1,2</sup> (Cy) and per-*O*-methylcyclohexaamylose.<sup>3</sup> Our results indicate preferential binding of the aromatic portions of these anions in binary complexes with per-*O*-methylcyclohexaamylose but the *p*-methylcinnamate anion is preferentially bound at the carboxylate terminal in the binary complex with Cy. In all cases, however, the substrate is located in the wide zone of the macrocycle cavity. All observed ternary complexes and the dimer aggregate of per-*O*-methylcyclohexaamylose involved binding at the wide aperture as well.

We now report <sup>13</sup>C NMR spectrometric evidence that in complexes with formic, acetic, and benzoic acids the substrates are included within the narrow zone of the Cy cavity. We have also sought to obtain reliable values for the thermodynamic parameters which describe these complexation reactions in order to gain some understanding of the nature of the binding forces in these complexes.

## pH Potentiometric Method

We have developed a novel means of measuring the Cy-guest complex formation constant when the guest species is a participant in an acid-base equilibrium. The method is based on the fact that the guest is effectively removed from the acid-base system by its complexation and, as a result, that system reacts to replenish the complexed species. If the guest is the conjugate base, then hydrogen ions are released into solution as acid dissociates to replenish the base lost in complexation. Conversely, hydrogen ions are removed from solution if the complexation guest is the acid. By measuring the pH as Cy is added, we are able to calculate the extent of Cy-guest complexation and, hence, the complex formation constant. Even if Cy forms complexes with both the acid and conjugate base, as is true with benzoate-benzoic acid mixtures, the method is capable of simultaneously determining both complexation equilibrium constants.

In the equations that follow we will make provision for both binary (CyB<sup>-</sup> and CyHB) and ternary (Cy<sub>2</sub>B<sup>-</sup> and Cy<sub>2</sub>HB) complexes of Cy with acid HB and conjugate base B<sup>-</sup>, although in any given case fewer than four types of complexes may exist. An aqueous solution is prepared containing analytical concentrations  $F_{HB}$  of the acid and  $F_{NaB}$  of the base (typically as the sodium salt) and having an initial volume  $V$ . This solution is thermostated and the pH is recorded. Then successive weighed portions of solid Cy are added and the pH is again recorded when equilibrium is reached after each addition. The model equations describing the equilibria and other

properties of each such solution follow.

B conservation equation in molar concentration units

$$F_B = F_{NaB} + F_{HB} = [B^-] + [HB] + [CyB^-] + [CyHB] + [Cy_2B^-] + [Cy_2HB] \quad (1)$$

Cy conservation equation in molar concentration units

$$F_{Cy} = [Cy] + [CyB^-] + [CyHB] + 2[Cy_2B^-] + 2[Cy_2HB] \quad (2)$$

charge conservation equation in molar concentration units

$$[H^+] + F_{NaB} = [B^-] + [CyB^-] + [Cy_2B^-] + [OH^-] \quad (3)$$

acid-base equilibrium

$$K_a' = \frac{K_a}{\gamma_H + \gamma_{B^-}} = \frac{[H^+][B^-]}{[HB]} \quad (4)$$

water dissociation equilibrium

$$K_w' = \frac{K_w}{\gamma_H + \gamma_{OH^-}} = [H^+][OH^-] \quad (5)$$

CyB<sup>-</sup> complex formation

$$K'_{CyB^-} = \frac{K_{CyB^-} \gamma_{B^-}}{\gamma_{CyB^-}} = \frac{[CyB^-]}{[Cy][B^-]} \quad (6)$$

CyHB complex formation

$$K_{CyHB} = \frac{[CyHB]}{[Cy][HB]} \quad (7)$$

Cy<sub>2</sub>B<sup>-</sup> stepwise formation

$$K'_{Cy_2B^-} = \frac{K_{Cy_2B^-} \gamma_{CyB^-}}{\gamma_{Cy_2B^-}} = \frac{[Cy_2B^-]}{[Cy][CyB^-]} \quad (8)$$

Cy<sub>2</sub>HB stepwise formation

$$K_{Cy_2HB} = \frac{[Cy_2HB]}{[Cy][CyHB]} \quad (9)$$

activity coefficient correlation (Debye-Hückel) for ionic species  $i$

$$\log \gamma_i = \frac{-B_1 I^{1/2}}{1 + B_2 a_i I^{1/2}} \quad (10)$$

where  $B_1$  and  $B_2$  are temperature-dependent parameters taken from the Robinson and Stokes<sup>4</sup> tabulation and ion size parameter values  $a_i$  are assumed to be 0.9, 0.35, 0.4, 0.4, 0.6, 1.6,<sup>2</sup> and 1.8<sup>2</sup> nm for H<sup>+</sup>, OH<sup>-</sup>, formate, acetate, benzoate, all CyB<sup>-</sup>, and all Cy<sub>2</sub>B<sup>-</sup>, respectively.

The addition of successive portions of solid Cy up to the

**Table I.** pH Potentiometric Determination of Binary Complex Formation Constants

temp, °C	formation constant	standard error	residual std dev
Cyclohexaamylose-Formic Acid $K_{CyHB}$			
15	4.37	0.08 <sup>a</sup>	0.0016
25	4.12	0.06 <sup>a</sup>	0.0008
30	4.06	0.07	0.0021
40	3.94	0.07	0.0022
50	3.10	0.06 <sup>a</sup>	0.0020
Cyclohexaamylose-Acetic Acid $K_{CyHB}$			
15	10.42	0.09	0.0040
25	9.17	0.09 <sup>a</sup>	0.0007
30	8.89	0.08 <sup>a</sup>	0.0013
40	8.10	0.59	0.0067
50	6.42	0.07 <sup>a</sup>	0.0015
Cyclohexaamylose-Benzoic Acid $K_{CyHB}$			
15	1397.	12.	0.0063
25	751.	1.	0.0020
30	583.	4.	0.0033
40	325.	2.	0.0042
50	203.	1.	0.0025
Cyclohexaamylose-Benzoate Ion $K_{CyB}$			
15	14.41	0.12 <sup>a</sup>	0.0063
25	10.51	0.05	0.0020
30	9.69	0.06	0.0033
40	8.10	0.06	0.0042
50	6.58	0.08	0.0025

<sup>a</sup> Standard error estimate of the formation constant is based on an a priori standard deviation of 0.002 for the measurements. All other standard errors are based on the residual standard deviation shown in the fourth column.

solubility limit of about 10 wt % Cy requires corrections to be applied to the solution volume and to the pH measurement. These corrections were determined by auxiliary experiments. One of these involved measuring the densities of aqueous Cy solutions and provides the empirical result that the total solution volume  $V_T$  increased linearly with the mass  $g_{Cy}$  of Cy according to

$$V_T = V + 0.7g_{Cy} \quad (11)$$

Consequently, the analytical concentrations were each reduced by the ratio  $V/V_T$  as Cy was added. The second correction compensated for any error induced by the Cy in the pH measurement. The presence of Cy, which does not itself have measurable acid-base properties in the pH region of interest, might affect pH measurement in two ways. Firstly, the addition of a high nonelectrolyte concentration might alter the solvent dielectric constant and thereby affect ionic activity coefficient values, and hence the apparent solution pH. Secondly, a source of error is the possible effect of Cy on the junction potentials at the glass electrode and reference electrode, solution interfaces. To distinguish between these phenomena and to find a suitable empirical correction method, we measured the pH of 0.1, 0.01, and 0.002 M HCl solutions upon stepwise addition of weighed Cy portions at 25 and at 50 °C. These measurements of  $pH_{obsd}$  were compared to the well-known pH values of aqueous HCl and were correlated empirically by

$$pH = pH_{obsd} + 0.55 \frac{g_{Cy}}{V_T} = -\log \gamma_{H^+}[H^+] \quad (12)$$

This same correlation was found for all three HCl concentrations to within the  $\pm 0.002$  pH precision of our measurements. From this we conclude that the main source of pH error is a change in the liquid junction potentials induced by Cy rather than changes in the dielectric constant with subsequent change

in activity coefficients. An activity coefficient effect would depend on the ionic strength and no such dependence was observed in the range 0.002–0.1 M.

Each measured  $pH_{obsd}$  was corrected according to eq 12 to yield hydrogen ion concentrations as if in the absence of Cy. The corrections did not exceed about 0.05 pH units in any case. Neither empirical correction in eq 11 or 12 was found to depend on temperature in any significant way.

The model equations 1–12 include as unknown parameters as many as five equilibrium constants (including  $K_a$  but excluding  $K_w$ ) if all four complexes actually form. In order to estimate statistical uncertainties we make more than the minimum number of measurements, at least 8 and as many as 11 at any given temperature for any particular acid-base system. The resulting equations then comprise an overdetermined, coupled, nonlinear set which is solved numerically using nonlinear regression techniques as described elsewhere.<sup>5</sup>

### pH Potentiometric Results

Measurements were made on formic, acetic, and benzoic acid systems between 15 and 50 °C. Both the formic and acetic acid systems data could be fitted adequately with  $K_{CyB}$ ,  $K_{Cy_2B}$ , and  $K_{Cy_2HB}$  fixed at zero. The benzoic acid system, however, required nonzero values of both  $K_{CyHB}$  and  $K_{CyB}$ . These observations confirm the expectations that Cy forms binary complexes with formic, acetic, and benzoic<sup>6</sup> acids and benzoate<sup>6</sup> ion but not with acetate or formate ion. Ternary complexes cannot be detected in these systems. Table I shows the complex formation constants and their uncertainties expressed as standard errors (square roots of the variance estimates). The fourth column in Table I lists the standard deviations of the residuals to the fitted curve and these may be compared to an expected statistical uncertainty of approximately 0.002 based on the pH measurement precision.

To obtain estimates of the maximum probable systematic error in the complex formation constants, we repeated the calculations, each time adjusting the experimental quantities by an amount that appeared to be a reasonable estimate of the maximum error in that value. As an example, we estimate the purity of the Cy reagent to be within 0.5% of 100% and this purity uncertainty is one of several sources of systematic error. The assumed 99.5% Cy purity was employed in calculating a new set of formation constants and these were compared with the previous values. This procedure was repeated with each imaginable source of systematic error. The maximum excursion due to systematic errors is  $\Delta K_{max} = \sum |\Delta K_i / \Delta x_i| \Delta x_i$  where each  $x_i$  is an experimental quantity like the Cy purity. The results appear at the bottom of Table II.

To find thermodynamic parameters  $\Delta H^\circ$  and  $\Delta S^\circ$  for the complexation reactions, we utilized the well-known relationships  $d \ln K / dT^{-1} = \Delta H^\circ / R$  and  $dT \ln K / dT = \Delta S^\circ / R$  together with the observed linearity of both  $\ln K$  vs.  $T^{-1}$  and  $T \ln K$  vs.  $T$  plots and calculated weighted least-squares lines of the data in Table I. Weighting factors were required because of the  $\ln K$  and  $T \ln K$  transformations of the measured dependent variable  $K$ . These weighting factors were inversely proportional to the variances of the transformed dependent variables and so were  $K^2 / \text{var}(K)$  for the  $\ln K$  vs.  $T^{-1}$  lines and  $K^2 / T^2 \text{var}(K)$  for the  $T \ln K$  vs.  $T$  lines, where  $\text{var}(K)$  values were the square of the standard error estimates in the third column of Table I. Before calculating these lines, we rejected two points as outliers and those were the 50 °C formic acid value, which is well off the line defined by the other four points, and the 40 °C acetic acid value, for which the fit was unacceptably poor indicating some undetected extreme systematic error. The thermodynamic parameters calculated in this manner are shown in Table III along with uncertainty estimates. Statistical uncertainties were calculated from the standard error estimates of the slopes of the least-squares lines.

**Table II.** Systematic Error Propagation for Potentiometric Measurement of Formation Constants of Cy with Acetic, Formic, and Benzoic Acids and Benzoate Anion

error source	error in formation constant, % <sup>a</sup>			
	acetic acid	formic acid	benzoic acid	benzoate ion
Cy reagent purity, $\pm 0.5\%$	0.4	0.3	0.7	1.3
anion concentration, $\pm 0.5\%$		0.1	0.2	0.2
acid concentration, $\pm 0.5\%$	0.1		0.4	0.6
pH meter standardization, measurement, $\pm 0.005$ pH units			0.2	0.3
volume correction <sup>b</sup>	0.6	0.2	0.2	0.6
pH correction <sup>c</sup>	2.7	4.3	0.7	3.5
activity coefficient correlation, ion size parameter				
H <sup>+</sup> , $\pm 0.1$ nm				
B <sup>-</sup> , $\pm 0.1$ nm		0.1		0.5
CyB <sup>-</sup> , $\pm 0.2$ nm				
totals	3.8	5.0	2.4	7.0

<sup>a</sup> Blank entries indicate changes in  $K$  of less than 0.05%. <sup>b</sup>  $V_T$  was obtained from  $V_T = V + 0.6g_{Cy}$  instead of eq 11. <sup>c</sup> The pH correction was calculated from  $pH = pH_{obsd} + 0.50g_{Cy}/V_T$  instead of eq 12.

**Table III.** Thermodynamic Parameters for Complex Formation Reactions

substrate	$\Delta S^\circ$ , cal mol <sup>-1</sup> K <sup>-1</sup>			$\Delta H^\circ$ , kcal mol <sup>-1</sup>		
	value	std error	max systematic error	value	std error	max systematic error
formic acid	+0.3	0.4	1.7	-0.74	0.11	0.6
acetic acid	-4.5	1.0	1.4	-2.68	0.03	0.5
benzoic acid	-20.9	0.5	0.8	-10.15	0.14	0.3
benzoate ion	-8.4	1.1	2.4	-3.9	0.3	0.8

**Table IV.** Estimates of Thermodynamic Parameters for Complex Formation Reactions of Cy with Acetic Acid, Benzoic Acid, and Benzoate Anion at 25 °C

substrate	log $K$	$\Delta H^\circ$ , kcal mol <sup>-1</sup>	$\Delta S^\circ$ , cal mol <sup>-1</sup> K <sup>-1</sup>
acetic acid	$0.962 \pm 0.004^a$ ( $\pm 0.020$ )	$-2.68 \pm 0.03$ ( $\pm 0.5$ )	$-4.5 \pm 1.0$ ( $\pm 1.4$ )
ref 7 <sup>b</sup>	$3.8 \pm 1.2$	$-1.2 \pm 0.1$	+13
benzoic acid	$2.876 \pm 0.0006^a$ ( $\pm 0.016$ )	$-10.15 \pm 0.14$ ( $\pm 0.3$ )	$-20.9 \pm 0.5$ ( $\pm 0.8$ )
ref 7 <sup>b</sup>	$3.0 \pm 0.1$	$-9.6 \pm 0.1$	-18
ref 6 <sup>c</sup>	$2.90 \pm 0.04$		
ref 8	3.02		
benzoate ion	$1.021 \pm 0.002^a$ ( $\pm 0.029$ )	$-3.9 \pm 0.3$ ( $\pm 0.8$ )	$-8.4 \pm 1.1$ ( $\pm 2.4$ )
ref 9 <sup>d</sup>	$1.09 \pm 0.08$		
ref 6 <sup>c</sup>	$0.99 \pm 0.11$		

<sup>a</sup> This work. Uncertainties given in parentheses represent maximum probable error estimates. <sup>b</sup> Uncertainties represent standard deviations of three or four runs. <sup>c</sup>  $I = 0.5$ , D<sub>2</sub>O solvent. <sup>d</sup>  $I = 0.2$ .

Estimates of the maximum systematic errors were found by standard error propagation techniques applied to  $\Delta K_{max}$  values to obtain maximum errors in the slopes of the lines which gave, in turn, error estimates for  $\Delta H^\circ$  and  $\Delta S^\circ$ . Table IV compares some of our results with those obtained elsewhere. The values of log  $K$  for benzoic acid and benzoate anion seem in rough agreement but our values with acetic acid are substantially different from those in ref 7. The large scatter reflected by a standard deviation of  $\pm 1.2$  log units may indicate some undetected systematic error in the earlier work. No comparable measurements have been reported for the formic acid system.

### <sup>13</sup>C NMR Spectrometric Measurements

The <sup>13</sup>C NMR spectra of 5% D<sub>2</sub>O (v/v, aqueous) solutions containing Cy and either formic, acetic, benzoic acid, or benzoate substrate consist of resonance lines corresponding to six nonequivalent carbons on Cy and the expected number of lines for each substrate species. Assignments of resonances of Cy and the substrates have been previously reported.<sup>10,11</sup> The

model equations and computational strategies for extracting intrinsic chemical shift parameters from the measured resonances have been reported in detail in an earlier communication.<sup>2</sup> Table V shows the results of these measurements and calculations. The symbolism used in that table and in the forthcoming discussion conforms to our earlier usage, i.e., a given carbon resonance is denoted by a superscript referring to the species and carbon in question while a subscript 0 or 1 refers to the uncomplexed species or the binary complex, respectively. For example,  $\delta_0^{(Cy6)}$  refers to carbon 6 in uncomplexed Cy,  $\delta_1^{(Cy6)}$  refers to carbon 6 in Cy in binary complex, and the displacement  $\Delta\delta_1^{(Cy6)}$  due to complexation is  $\delta_1^{(Cy6)} - \delta_0^{(Cy6)}$ .

The discussion which follows is divided into three main sections, the first of which deals with formic and acetic acid complexes of Cy, the second with the Cy-benzoic acid complex, and the concluding section with the benzoate complex. In each case, we will restrict the discussion to a single binding mode which seems to us to best fit the observed patterns of resonance displacements. This restriction is not meant to imply that other

Table V.  $^{13}\text{C}$  NMR Chemical Shifts<sup>a</sup> and Their Displacements Due to Complexation with Substrates

		Cyclohexaamylose Carbon Resonances			
Cy carbon	$\delta_0(\text{Cy})$	$\Delta\delta_1(\text{Cy})$			
		formic acid	acetic acid	benzoic acid	benzoate
1	102.39	0.05	0.16	0.46	0.22
2	72.86	0.10	0.01	0.11	0.18
3	74.46	0.10	0.15	0.24	-0.02
4	82.25	-0.08	-0.07	0.04	0.12
5	73.04	-0.36	-0.26	-0.39	0.31
6	61.58	-0.24	-0.31	-0.44	0.05
std error	$\pm 0.02$	$\pm 0.04$	$\pm 0.04$	$\pm 0.03$	$\pm 0.06$
rms fit <sup>b</sup>		0.08	0.02	0.02	0.01

		Substrate Carbon Resonances						
substrate carbon	formic acid		acetic acid		benzoic acid		benzoate	
	$\delta_0(\text{HB})$	$\Delta\delta_1(\text{HB})$	$\delta_0(\text{HB})$	$\Delta\delta_1(\text{HB})$	$\delta_0(\text{HB})$	$\Delta\delta_1(\text{HB})$	$\delta_0(\text{B})$	$\Delta\delta_1(\text{B})$
$\alpha$					171.97	-1.70	176.62	-0.76
1	166.88	-0.21	177.78	-2.45	130.91	-1.18	137.33	0.49
2			1.52	0.48	130.64	1.59	129.84	0.52
3					129.74	-0.76	129.34	-0.25
4					134.72	0.93	132.24	-0.65
std error	$\pm 0.02$	$\pm 0.15$	$\pm 0.01$	$\pm 0.07$	$\pm 0.03$	$\pm 0.05^c$	$\pm 0.02$	$\pm 0.07$
rms fit <sup>b</sup>		0.02	0.02		0.03		0.01	

<sup>a</sup> Chemical shifts are relative to  $\text{Me}_4\text{Si}$ . Upfield displacements are negative. <sup>b</sup> rms fit =  $(\sum(\delta_{\text{calcd}} - \delta_{\text{obsd}})^2/n)^{1/2}$ . <sup>c</sup> Benzoic acid carbon chemical shifts standard errors are based on 0.03 ppm precision of the measurements. All others assume 0.02 ppm. <sup>d</sup> Assignments may be reversed for benzoate ion.

structures cannot exist. It is possible that some such structures are present in minor concentrations and do, indeed, contribute to the observed  $^{13}\text{C}$  displacements.

**Formic and Acetic Acid Complexes.** Similar upfield displacements of carboxylic acid carbons in formic and acetic acid ( $-2.1 \pm 0.15$  and  $-2.45 \pm 0.07$  ppm, respectively) result from insertion of these molecules into the Cy cavity in their respective complexes. Substantial and nearly identical Cy displacements at C5 and C6 ( $-0.36 \pm 0.06$ ,  $-0.24 \pm 0.06$  and  $-0.26 \pm 0.04$ ,  $-0.31 \pm 0.04$  ppm for C5, C6 in formic and acetic acid complexes, respectively) seem to indicate that the substrates are localized in the narrow rim of the Cy activity, which we define here as the tail of the molecule. This conclusion is supported by the rather small perturbations at the C2 and C3 sites at the wide rim of the cavity. The  $^{13}\text{C}$  NMR resonance displacements at these carbons (0.10, 0.10 and 0.01, 0.15 ppm in formic and acetic acids, respectively) are to be contrasted both with the larger displacements at C5 and C6 here and with  $^{13}\text{C}$  NMR displacements observed in binary and ternary complexes of Cy with *p*-methylcinnamate anion.<sup>2</sup> C2 and C3 displacements in the binary *p*-methylcinnamate complex, which involved insertion of the carboxylate terminal of the anion into the wide Cy rim, were 0.2 and 0.4 ppm, respectively. The ternary complex was assigned a structure in which the anion is occluded between two Cy molecules in a head to head orientation and has displacements of 0.32 and 0.67 ppm at C2 and C3, respectively. C5 and C6, which do not interact with the substrate in the ternary *p*-methylcinnamate, Cy complex, are perturbed only to the extent of 0.00 and  $-0.05$  ppm. These comparisons lead us to propose a structure in which these substrates are held in the tail of the Cy molecule which is defined by the band of C5 and C6 carbon atoms.

**Benzoic Acid Complex.** The upfield displacement of benzoic acid's carboxylic acid carbon, C $\alpha$ , is somewhat smaller than that noted with formic and acetic acids and this may be ascribable to the attenuating effect of the aromatic system. The observed alternating pattern of displacements in the phenyl ring carbons is consistent with this behavior. In any case, it seems clear that the carboxylic acid terminal of benzoic acid undergoes the primary interaction with Cy in the complex. Bergeron, Channing, and McGovern<sup>6</sup> recently measured the

intermolecular nuclear Overhauser effect with the benzoic acid-Cy complex and determined that this effect was much more pronounced at the C2 (ortho) hydrogen of benzoic acid than at the C3 (meta) position and concluded, as we do, that the charge-rich carboxylic acid group is inserted into the Cy cavity.

Displacements of Cy  $^{13}\text{C}$  NMR resonances in the complex suggest that the carboxylic acid group is inserted in the narrow rim tail of the Cy molecule as is evidenced by the large displacement noted at C6 ( $-0.44$  ppm). Displacements of other Cy carbon resonances in this system follow the same pattern as those observed with both formic and acetic acids but are consistently larger. Presumably, this reflects stronger host-guest interactions as indicated also by the more negative  $\Delta H^\circ$  value found in the benzoic acid complex formation.

Our interpretation differs from that of Bergeron et al.,<sup>6</sup> who describe a structure in which benzoic acid enters the Cy cavity from the C2, C3 wide rim. Their conclusions are based, first, on the large displacements noted in C3 and C5 proton resonances in  $^1\text{H}$  NMR experiments and, second, on the lack of a displacement of C6 hydrogen atoms. Since either the "head" structure or the "tail" structure would allow for displacements of both  $^{13}\text{C}$  NMR and  $^1\text{H}$  NMR resonances at C5, the behavior at C3 and C6 seems critical. To aid in visualizing the host-guest interactions, we assembled space-filling models of the two suggested structural isomers of the complex. The "head" structural model featured atom proximities which suggest that large perturbations should be noted in the  $^{13}\text{C}$  NMR signals of C2, C3, and C5 but that C6 resonances should be nearly unaffected. This pattern of displacements was not noted in our  $^{13}\text{C}$  NMR work. The "head" model was consistent with large  $^1\text{H}$  displacements at C3 and C5 as observed by Bergeron et al. The model suggested that the C6 proton interaction with the substrate depended critically on the populations of rotameric conformers at C6. These protons experience a differing set of interactions with neighboring Cy atoms and with the substrate depending on rotameric form. Consequently we could draw no conclusions about  $^1\text{H}$  displacements at C6. In the "tail" structural model in which the carboxylic acid group is inserted at the C5, C6 end of Cy, most of the length of the benzoic acid molecule could penetrate the cavity.

Proximity of C5 and C6 to the substrate suggested substantial perturbations of these  $^{13}\text{C}$  NMR signals and the C5 proton would probably be substantially perturbed as well. However, the complexity of interactions which might be experienced by different rotameric forms of the C6 protons did not seem to allow a firm prediction. We also noted that the carboxylic acid oxygen atoms were very close to the C3 proton and so would be expected to cause substantial displacements in the  $^1\text{H}$  NMR signal and in the C3 resonance of the  $^{13}\text{C}$  NMR spectrum.

In summary, the "tail" model of the complex is consistent with the observed large  $^{13}\text{C}$  NMR displacements at C5 and C6 as well as the observed 0.24-ppm displacement at C3. This structure is consistent with the  $^1\text{H}$  NMR spectral data as well in that large displacements of C3 and C5 proton resonances are predicted. The small displacements of C6 proton resonances may be explained by changes in the rotameric C6 conformations upon inclusion of the substrate. However, the "head" model of the complex is inconsistent with the  $^{13}\text{C}$  NMR displacement data and does not seem to reflect the actual structure of the complex.

**Benzoate Complex.** The pattern of benzoate  $^{13}\text{C}$  NMR displacements in this system differs markedly from those encountered with both the benzoic acid complex and complexes of *p*-methylcinnamate anion with Cy. The small  $\text{C}\alpha$  displacement observed here ( $\Delta\delta_1(\text{B}\alpha) = -0.76 \pm 0.06$  ppm) is to be compared with an upfield displacement of about 3 ppm which we have noted for *p*-methylcinnamate and 4-biphenylcarboxylate complexes in which the terminal carboxylate group is preferentially bound in the Cy cavity. It appears likely that the benzoate complex is one, by contrast, in which the phenyl terminal is preferentially bound in the Cy cavity.

Cy resonance displacements seem to indicate insertion of the benzoate ion into the wide C2, C3 rim of the molecule in that the C6 resonance is not appreciably displaced ( $\Delta\delta_1(\text{C}y6) = 0.05 \pm 0.06$  ppm) but the resonance at C2 is somewhat larger ( $\Delta\delta_1(\text{C}y2) = 0.18 \pm 0.06$  ppm). It is noteworthy, in this regard, that Bergeron et al.<sup>6</sup> measured a large upfield displacement in the proton resonance at C3 of Cy but our data indicate only a minor displacement, if any, of the C3 carbon resonance ( $\Delta\delta_1(\text{C}y3) = -0.02 \pm 0.06$  ppm). Apparently, in this case the C3 proton is much more strongly affected by the presence of a substrate than is the C3 carbon atom. The  $^1\text{H}$  NMR data seem to indicate, in agreement with our conclusion, that the benzoate anion is bound at the head of the Cy molecule.

A substantial displacement of the C5 resonance ( $\Delta\delta_1(\text{C}y5) = -0.31 \pm 0.06$  ppm) supports the phenyl-insertion model as follows. The C5 carbon atom is at the tail of the Cy cavity, so in order to be noticeably perturbed must experience close proximity with the bound substrate and, as a consequence, the substrate must penetrate deeply into the Cy cavity. If the carboxylate terminal of benzoate were to penetrate the cavity to the extent of perturbing C5 in Cy, the carboxylate carbon would experience a large perturbation which would be reflected in a  $\Delta\delta_1(\text{B}\alpha)$  value near  $\sim -3$  ppm. Because this is not observed, binding in the benzoate complex appears to involve phenyl insertion into the wide Cy rim.

#### Discussion of the Thermodynamic Data

$\Delta H^\circ$  and  $\Delta S^\circ$  values have been measured for relatively few Cy-substrate complex formation reactions, so that conclusions based on these data must remain tentative. However, we have noted several interesting trends in our results. The first of these is the apparent proportionality of  $\Delta H^\circ$  and  $\Delta S^\circ$  values in the systems we have measured. To the four complexes we have investigated here we add the ternary Cy-4-biphenylcarboxylate complex with  $\Delta H^\circ = -28 \pm 2$  kcal mol $^{-1}$  and  $\Delta S^\circ = -72 \pm 6$  cal mol $^{-1}$  K $^{-1}$ .<sup>1</sup>

The second trend we note is an apparent correspondence

between the  $\Delta H^\circ$ ,  $\Delta S^\circ$  set and the  $^{13}\text{C}$  NMR displacements at C1. Displacements of these carbon resonances are generally ascribed to conformational changes about interglucosyl linkages in Cy.<sup>10</sup> For formic and acetic acids, benzoate ion, and benzoic acid,  $\Delta S^\circ$  values for the complex formation reactions are +0.3, -4.5, -8.4, and -20.9 cal mol $^{-1}$  K $^{-1}$ , respectively. Noting that the ternary Cy-4-biphenylcarboxylate complex involves 2 mol of Cy for each mol of complex,  $\Delta S^\circ = -36$  cal (mol Cy) $^{-1}$  K $^{-1}$ . These entropy changes seem to have more than an accidental correspondence with the observed C1 displacements, which are 0.05, 0.16, 0.22, 0.46, and 0.75 ppm, respectively. One obvious conclusion which may be drawn from this trend is that increasing conformational change in the Cy system results in loss of rotational and vibrational freedom in the macrocyclic molecule and this in turn is responsible for increasingly negative  $\Delta S^\circ$  values. The fact that these trends are observed with complexes of differing structures, and with both neutral and ionic substrates, seems to suggest that changes in Cy entropy are the main source of entropy change in the complexations. Presumably, the extent of conformational change in a given complex is determined by the strength of the bonding interaction as reflected by the value of  $\Delta H^\circ$ . Thus strong bonding interactions apparently cause large conformational changes which result in decreased system entropy. While such an explanation might seem appealing, it must remain speculative at present.

#### Experimental Section

Formate-formic acid, acetate-acetic acid, and benzoate-benzoic acid solutions (typically 0.01 F HB and 0.01 F B $^-$ ) were prepared by addition of suitable amounts of standard NaOH to stock solutions of the acids. The resulting mixtures were assayed for acid by NaOH titration. All other reagents were prepared from reagent grade commercial samples and used without further purification. Cyclohexaamylose was obtained as the commercial tetrahydrate.  $^{13}\text{C}$  NMR spectra which were obtained over extremely long acquisition times to maximize *S/N* (>200) indicated negligible impurity concentrations. pH measurements with even 0.1 M Cy solutions in water gave no indication of acidic or basic impurities.

An Orion 801 pH meter equipped with conventional glass and reference electrodes was employed in pH measurements. In a typical experiment, the meter was standardized against 0.05 *m* potassium hydrogen phthalate thermostated at the appropriate temperature after about 30 min equilibration time. A portion of the acid-conjugate base solution was added to the thermostated cell and an initial pH was recorded after about 30 min of standing time. Weighed portions of Cy were added to the stirred contents of the cell and pH readings were obtained after equilibration, typically lasting 2-3 min. In some experiments a nitrogen purge was employed at several points during the Cy addition but the pH was entirely unaffected and so this procedure was omitted in subsequent work. After most experiments the pH standardization was rechecked and never varied by more than 0.003 pH units.

$^{13}\text{C}$  nuclear magnetic resonance spectra employed a Varian CFT-20 spectrometer equipped with a 10-mm sample tube maintained at  $30 \pm 2$  °C. All spectra were obtained with 5% D $_2$ O solvent but analyte solutions and instrumental settings were similar to those used in earlier work.<sup>1,2</sup>

**Acknowledgment.** We thank Professor Elkan R. Blout for providing access to the CFT-20 spectrometer at the Department of Biological Chemistry at the Harvard Medical School. This work was supported in part by a research grant from the National Institute of General Medical Sciences, U.S. Public Health Service (GM26004).

#### References and Notes

1. R. I. Gelb, L. M. Schwartz, C. T. Murray, and D. A. Laufer, *J. Am. Chem. Soc.*, **100**, 3553 (1978).
2. R. I. Gelb, L. M. Schwartz, and D. A. Laufer, *J. Am. Chem. Soc.*, **100**, 5875 (1978).
3. R. I. Gelb, L. M. Schwartz, J. E. Markinac, and D. A. Laufer, *J. Am. Chem.*

- Soc., preceding paper in this issue.
- (4) R. A. Robinson and R. H. Stokes, "Electrolyte Solutions", 2nd ed., Butterworths, London, 1965.
- (5) L. M. Schwartz and R. I. Gelb, *Anal. Chem.*, **50**, 1571 (1978).
- (6) R. J. Bergeron, M. A. Channing, and K. A. McGovern, *J. Am. Chem. Soc.*, **100**, 2878 (1978).
- (7) E. A. Lewis and L. D. Hansen, *J. Chem. Soc., Perkin Trans. 2*, 2081 (1973).

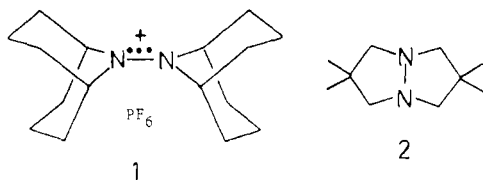
- (8) B. Casu and L. Rava, *Ric. Sci.*, **36**, 733 (1966).
- (9) R. L. Van Etten, J. F. Sebastian, G. A. Clowes, and M. L. Bender, *J. Am. Chem. Soc.*, **89**, 3242 (1967).
- (10) P. Colson, H. J. Jennings, and I. C. P. Smith, *J. Am. Chem. Soc.*, **96**, 8081 (1974).
- (11) E. Wenkert, B. L. Buckwalter, I. R. Burflitt, M. J. Gasic, H. E. Gottlieb, E. W. Hageman, F. F. Schell, and P. M. Wovkulich in "Topics in Carbon-13 NMR Spectroscopy", Vol. 2, G. Levy, Ed., Wiley, New York, 1976.

## Communications to the Editor

### Twisted and Bent Hydrazine Radical Cations

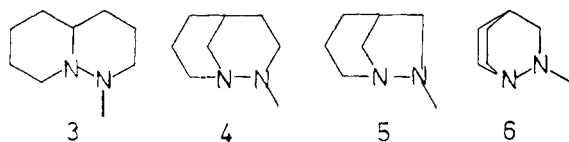
Sir:

The recent X-ray structure determination of bis(9-azabicyclo[3.3.1]nonane) radical cation hexafluorophosphate (**1**) showed that this hydrazine radical cation has an olefin-like structure.<sup>1</sup> The four  $\alpha$  carbons are coplanar with the nitrogens,



formally leaving pure p-hybridized orbitals to bear the three  $\pi$  electrons, and the N-N bond length is surprisingly short at 1.269 (7) Å. Electrochemical<sup>2</sup> and ESR<sup>3</sup> studies are also consistent with an olefin-like geometry for other tetraalkylhydrazine radical cations, although modest amounts of bending at nitrogen are facile, and, if the alkyl groups destabilize a planar structure, as for **2**, the equilibrium geometry is nonplanar at N.<sup>3a</sup> In this work, the destabilization resulting when a tetraalkylhydrazine radical cation is forced to be twisted at the N-N bond or strongly pyramidal at nitrogen is estimated by measuring changes in  $E^\circ'$ , the standard potential of the hydrazine-hydrazine radical-cation couple (room temperature, in acetonitrile containing 0.1 M sodium perchlorate as supporting electrolyte, vs SCE for the work reported here). This allows determination of the difference in the hydrazine-hydrazine radical-cation free-energy gap for strained and unstrained examples.

Compounds **3-6** are a good series for study of the effect of introducing twisting strain into a hydrazine radical cation. All



have one methyl and three alkyls of similar size substituted on the hydrazine unit; so in the absence of twisting effects they would be expected to show quite similar  $IP_1$  and  $E^\circ'$  values. These data are summarized in Table I. The lone-pair peak separation of 1.04 eV, measured by photoelectron spectroscopy (PES), observed for **3** is as expected for the trans-fused, axial methyl conformation **3e(ea)**, known to be the major confor-

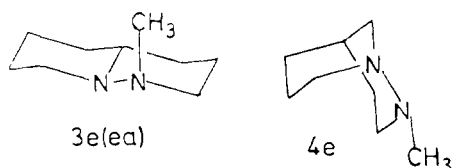


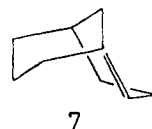
Table I. Photoelectron Spectroscopic and Electrochemical Data

compd	PES data	$E^\circ'$ <sup>a</sup>	$\Delta E^\circ'$ , kcal/mol <sup>b</sup>
Et <sub>2</sub> NNMeEt	8.02, 8.52	+0.25	+0.2
<b>3</b>	7.70, 8.74	+0.22	+0.6
<b>4</b>	7.69, 8.70, 9.12	+0.25	+1.3
<b>5</b>	8.18, 8.83	+0.68	+9.5
<b>6</b>	8.02, 8.53 <sup>c</sup>	irrev <sup>b</sup>	
<b>8</b>	7.63	+0.76	+13.8
<b>10</b>	8.12 <sup>d</sup>	+0.36 <sup>d</sup>	+2.4

<sup>a</sup> In CH<sub>3</sub>CN containing 0.1 M NaClO<sub>4</sub> as supporting electrolyte, vs. SCE, at 23 ± 1 °C. <sup>b</sup> See text. <sup>c</sup> From ref 7. <sup>d</sup> From ref 3c.

mation in solution from low-temperature NMR studies.<sup>4</sup> A distinct peak for  $IP_2$  of the **3e(ee)** conformation was not observed, but the onset of  $\sigma$  ionizations obscures the region in which it should appear. At least two conformations are occupied for **4**,<sup>5</sup> the major one showing  $IP_2 - IP_1$  of 1.01 eV, and a minor one with a 1.4-eV splitting. Which conformations are involved is not clear from our data, although the major one seems likely to be the chair-chair **4e** conformation.<sup>6</sup> A significantly larger  $IP_2 - IP_1$  difference was found for **5** than for **6**.

Hydrazine  $E^\circ'$  values show a weak dependence on  $IP_1$ , and we shall discuss the strain effects in terms of  $\Delta E^\circ'$  (kcal/mol) = 23.06 ( $E^\circ'$  (obsd, V) -  $E^\circ'$  (correln, V)), where  $E^\circ'$  (correln, V) = -0.961 + 0.15  $IP_1$ , as discussed previously.<sup>2c</sup>  $\Delta E^\circ'$  is defined as 0 for tetramethylhydrazine, is negative when  $E^\circ'$  is smaller than the correlation line predicts (as when the alkyl groups are tied back, for example in 1,1'-bispyrrolidine; so alkyl-alkyl interaction in the cation radical is smaller than in tetramethylhydrazine radical cation), and positive when  $E^\circ'$  is larger (as when steric interactions in the cation radical are larger than those between the methyls of tetramethylhydrazine radical cation).  $\Delta E^\circ'$  is larger for **3** than for triethylmethylhydrazine, as expected because of the strain introduced upon flattening at the nitrogens of the six-membered rings.<sup>2b,c</sup>  $\Delta E^\circ'$  for **3** should be a good model for that expected for **4** in the absence of twisting or bending effects in **4<sup>+</sup>**. The  $\Delta E^\circ'$  of **4** is <1 kcal/mol higher than that of **3**. This might be considered surprising considering the olefin-like geometry of hydrazine radical cations and the 12-kcal/mol strain found by Lesko and Turner<sup>8</sup> for the bridgehead olefin **7** compared with an acyclic model. The strain in **7** is not twisting



strain, however, but bending strain, and the small  $\Delta E^\circ'$  for **4** corroborates the less quantitative conclusion from the ESR work<sup>3</sup> that hydrazine radical cations are easily bent at nitrogen.